Anomalous elastic softening of $SmRu_4P_{12}$ under high pressure

Peijie Sun, Yoshiki Nakanishi, Mitsuteru Nakamura, and Masahito Yoshizawa*
Graduate School of Engineering, Iwate University, Morioka 020-8551, Japan

Masashi Ohashi and Gendo Oomi
Department of Physics, Kyushu University, Fukuoka 810-8560, Japan

Chihiro Sekine and Ichimin Shirotani
Faculty of Engineering, Muroran Institute of Technology, Muroran 050-8585, Japan

The filled skutterudite compound $SmRu_4P_{12}$ undergoes a complex evolution from a paramagnetic metal (phase I) to a probable multipolar ordering insulator (phase II) at $T_{MI} \sim 16.5$ K, then to a magnetically ordered phase (phase III) at $T_N \sim 14$ K. Elastic properties under hydrostatic pressures were investigated to study the nature of the ordering phases. We found that distinct elastic softening above T_{MI} is induced by pressure, giving evidence of quadrupole degeneracy of the ground state in the crystalline electric field. It also suggests that quadrupole moment may be one of the order parameters below T_{MI}. Strangely, the largest degree of softening is found in the transverse elastic constant C_T at around $0.5-0.6$ GPa, presumably having relevance to the competing and very different Grüneisen parameters Ω of T_{MI} and T_N. The interplay between the two phase transitions is also verified by the rapid increase of T_{MI} under pressure with a considerably large Ω of 9. These results can be understood on the basis of the proposed octupole scenario for $SmRu_4P_{12}$.

I. INTRODUCTION

$SmRu_4P_{12}$ is one of the more interesting members of the family of filled skutterudite RT_4X_{12} compounds (R=rare earths; T=Fe,Ru,Os; X=P,As,Sb). $SmRu_4P_{12}$ shows a variety of physical properties including superconductivity, metal-insulator (MI) transition, magnetic ordering, and heavy fermions (HFs).[1–3] The interest in $SmRu_4P_{12}$ is due to its MI transition at $T_{MI} \sim 16.5$ K, a subsequent antiferromagnetic transition at $T_N \sim 14$ K,[3] and a strange H-T magnetic phase diagram.[4,5] T_N is obscure at lower magnetic fields; however, it is distinctly visible in several measurements such as thermal expansion[6] even in a zero magnetic field. With increasing magnetic field, T_{MI} increases while T_N decreases, resembling CeB_6, which has an antiferroquadrupolar (AFQ) ordering and a subsequent magnetic ordering.[7] For this reason, $SmRu_4P_{12}$ was initially thought to be an AFQ system; however, increasing doubt is being thrown on this view, stimulating interest in the order parameters (OPs). $SmRu_4P_{12}$ crystallizes in a cubic structure with space group $Im\bar{3}$ (T_h^5), like other filled skutterudite compounds. Magnetic measurements show that Sm is trivalent with total angular momentum $J=5/2$. Specific-heat measurements suggest a crystalline electric-field (CEF) scheme consisting of a Γ_{67} ground-state quartet and an excited doublet Γ_5 at about 60 K in the T_h symmetry.[4,8] This scheme is plausible for understanding other measurements including the elastic constant.[9,10] Noticeably, the Γ_{67} quartet with both orbital and magnetic degeneracies is a key point for understanding the various properties of $SmRu_4P_{12}$. In this work, hydrostatic pressures of about 1 GPa are assumed to have no substantial effects on the CEF scheme.

The AFQ scenario for $SmRu_4P_{12}$ is under question as to several aspects. First, almost no elastic softening is observed above T_{MI} (Ref. 9) and the elastic anomaly at T_{MI} is not very large, unlike a typical AFQ ordering such as in CeB_6 (Ref. 11) and DyB_2C_2 (Ref. 12). Second, by application of magnetic fields, the specific-heat anomaly of AFQ ordering in CeB_6 is enhanced, while that at T_{MI} in $SmRu_4P_{12}$ changes only slightly; meanwhile, the anomaly at T_N in CeB_6 is weakened, whereas it is enhanced in $SmRu_4P_{12}$.[7,13] Recently, the possibility of octupole ordering was proposed for the MI transition.[14] This proposition is based on the appearance of elastic softening in phase II toward T_N and the indistinctness of the subsequent magnetic ordering at T_N, because these facts suggest a new coupling of $\Psi M \epsilon$ (Ψ, probable octupole OP in phase II; M, dipole OP in phase III; ϵ, elastic strain induced by ultrasound) and indicate breakdown of the time-reversal symmetry (TRS) in phase II. Breakdown of TRS is confirmed by muon spin relaxation,[15] nuclear magnetic resonance,[16] and Sm nuclear resonant scattering[17] measurements. An AFQ ordering is nonmagnetic and holds TRS, so is ruled out as the primary OP in phase II. On the other hand, an octupole ordering is magnetic and breaks TRS, so is possible in phase II. Microscopic measurements also suggest the appearance of magnetic dipole moment in phase II even in a zero magnetic field, in addition to an unknown multipole ordering.[16,17] This is very different from the strong candidate for octupole ordering material, NpO_2,[18] which has only one phase transition.

An isostructural compound, $PrRu_4P_{12}$, also shows a MI transition ($T_{MI} \simeq 63$ K).[19] Its MI transition is accompanied by no magnetic anomaly, whereas a distinct magnetic anomaly is observed in $SmRu_4P_{12}$. Moreover, a structural distortion is observed in $PrRu_4P_{12}$ (Ref. 20) but is absent in $SmRu_4P_{12}$. These facts indicate a magnetic origin for the MI transition in $SmRu_4P_{12}$, unlike $PrRu_4P_{12}$. In fact, a charge-density wave due to Fermi-surface nesting is plausible for interpreting the MI transition in $PrRu_4P_{12}$.[21] Recent x-ray

and polarized neutron diffraction experiments have shown that the Pr-ion site splits into two nonequivalent crystallographic sites. These experiments suggest two different CEF schemes below T_{MI},[22] where the importance of the *p-f* hybridization in the MI transition is also emphasized.

Ultrasonic measurement under hydrostatic pressures is rarely performed, partly due to its difficulty. We succeeded, however, in obtaining stable ultrasonic echoes by selecting a suitable sample of sufficient length. By performing such measurements, we intend to gain an insight into the following peculiarities in SmRu$_4$P$_{12}$. (1) The Γ_{67} quartet ground state degenerates with respect to Γ_3- and Γ_5-type quadrupole moments; however, no distinct elastic softening is observed at ambient pressure. Application of hydrostatic pressures is expected to induce stronger quadrupole-strain and intersite quadrupole interactions, which then affect elastic properties. Quadrupolar ordering, if visible under pressure, is helpful in understanding the possible OPs below T_{MI} and the peculiar *H-T* phase diagram. (2) We intend to build a pressure-temperature (*P-T*) phase diagram from which we can gain knowledge of the OPs of phases II and III. (3) One more point of interest is the very different Grüneisen parameters Ω of T_{MI} and T_N, the latter being much larger than the former.[23] Widely different Grüneisen parameters suggest different pressure dependencies of the two phase transitions; this prompted us to explore the physical properties under hydrostatic pressures related to this phenomenon.

II. EXPERIMENTS

A cylindrical polycrystalline SmRu$_4$P$_{12}$ sample, 4.1 mm in length and 3.4 mm in diameter, was employed. It was the same as the one used for ultrasonic measurements in magnetic fields[9] and was prepared at high temperatures and pressures using a wedge-type cubic anvil high-pressure apparatus. Actually, a single crystal was preferred, but the available single crystals at the time were very small, with dimensions of only $1 \times 1 \times 1$ mm^3, preventing us from obtaining stable ultrasonic echoes under high pressures.

The relative change of sound velocity v was measured by means of a phase-comparison technique. This technique measures the relative $\Delta v/v$ by detecting the relative frequency change $\Delta f/f$ while keeping the phase shift at zero and neglecting any changes in sample length $\Delta l/l$ (to be explained later). Elastic constant C is related to sound velocity v by the equation $C = \rho v^2$, where the density ρ of SmRu$_4$P$_{12}$ is 5.921 g cm^{-3}. LiNbO$_3$ piezoelectric plate with fundamental resonance frequency of $5-20$ MHz was used as the ultrasonic transducer to generate or detect the ultrasound. The only experimentally accessible ultrasound modes for a polycrystalline sample, i.e., longitudinal C_L propagating parallel to polarization and transverse C_T propagating perpendicular to polarization, were measured as a function of temperature under different hydrostatic pressures. The absolute values of C_L, C_T, and bulk modulus C_B of SmRu$_4$P$_{12}$ at 100 K are 153, 24.6, and 120 GPa, respectively.[9]

Hydrostatic pressure up to 1.15 GPa was generated using a Cu-Be piston-cylinder pressure cell and a Teflon capsule inside it. The cell has two layers: an outer cylinder and an
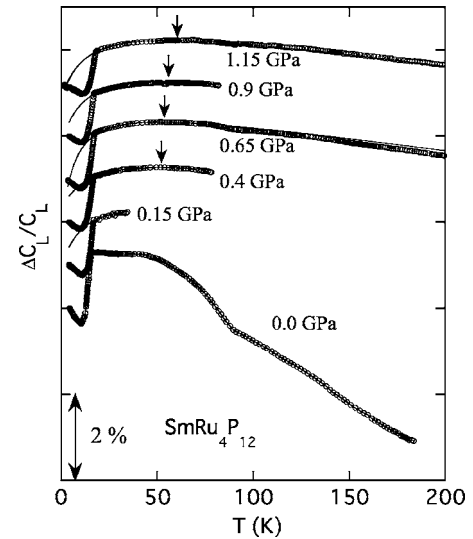

FIG. 1. Temperature dependence of the longitudinal elastic constant C_L under various pressures. The solid lines are the curves calculated by Eq. (3). The arrows indicate T_{soft} below which elastic softening appears.

inner one. The inner diameter and the length of the inner cylinder are 8 and 40 mm, respectively. The sample with two ultrasonic transducers bonded to it, together with a tin manometer, was placed in the Teflon capsule filled with a pressure medium (a 1:1 mixture of Fluorinert FC 70 and FC 77). The measurements were carried out down to the temperature of liquid helium, 4.2 K, or down to $\sim$1.5 K by pumping. The effective hydrostatic pressure inside the Teflon capsule was calibrated by measuring the superconducting transition temperature of the tin manometer.

III. EXPERIMENTAL RESULTS

Figure 1 shows the temperature dependence of the longitudinal mode $\Delta C_L/C_L$ under various pressures. The solid lines are fitted curves that will be explained later. The C_L at ambient pressure increases upon cooling down to T_{MI} without elastic softening. Application of hydrostatic pressures induces a clear softening above T_{MI}, but its pressure dependence is very weak. This may be partially due to the relative hardness of C_L that includes bulk modulus C_B. The temperature T_{soft}, below which softening appears, shows a slight increase with increasing pressure.

Figure 2 shows the temperature dependence of the transverse mode $\Delta C_T/C_T$ at various pressures, together with the fitted curves. Ambient pressure evidences a weak elastic softening above T_{MI} up to 35 K. With increasing pressure up to 0.6 GPa, elastic softening becomes increasingly marked. Furthermore, T_{soft} increases from 35 K for 0 GPa to about 80 K for 0.6 GPa. Strangely, upon further increasing the pressure by 0.7 GPa, the elastic softening fades again, while at the same time, T_{soft} also decreases. This strange pressure dependence presumably reflects the complexity of the phase diagram with two competing phase transitions. A kink structure is observed at around 90 K in both C_T and C_L at ambient pressure, reminiscent of the off-center motion of the *R* ions
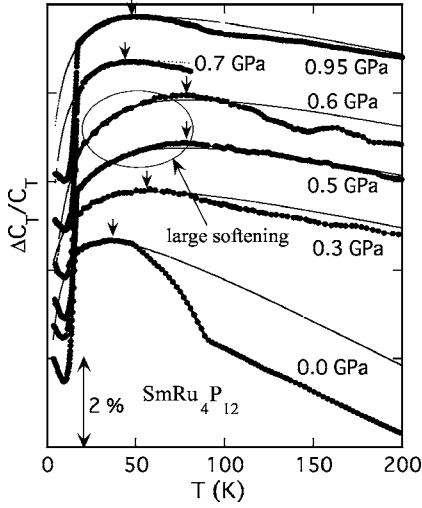
FIG. 2. Temperature dependence of the transverse elastic constant C_T under various pressures. The solid lines and arrows denote the same as in Fig. 1.

in the pnictogen cage, namely, "rattling," as in PrOs₄Sb₁₂.[24] However, here it seems to be not due to an intrinsic origin because it is absent in single crystals. The kink becomes very weak or undetectable as soon as even a relatively weak pressure is applied; this is also not expected for a rattling motion.

For both C_L and C_T, a distinct slope change in the background C^0 is noticeable, i.e., the lattice contribution to elastic constant before and after applying pressure. As for the reasons, the influence of pressure-induced sample length variation $\Delta l/l$, which alters the relative ultrasound velocity as follows, is possible:

$$\frac{\Delta v}{v} = \frac{\Delta f}{f} - \frac{\Delta \varphi}{\varphi} + \frac{\Delta l}{l}. \tag{1}$$

Equation (1) shows that in the phase-comparison technique, relative sound velocity $\Delta v/v$ is composed of three parts, e.g., the relative frequency $\Delta f/f$, relative signal phase $\Delta \varphi/\varphi$, and sample length $\Delta l/l$. $\Delta \varphi/\varphi$ is kept at zero by a feedback loop that compares the phase shift between the ultrasonic signal transported by the sample and the reference signal. $\Delta l/l$ is usually negligibly small. Therefore, this equation also explains why ultrasonic velocity v is measured as a shift in frequency. If $\Delta l/l$ induced by pressure accounts for the change in C^0, the linear-thermal-expansion coefficient $\alpha(T)$ is anticipated to be a change over 5×10^{-5} K⁻¹ under a pressure of about 0.3 GPa, in comparison with that at ambient pressure. This is at least an order of magnitude greater than the $\alpha(T)$ at ambient pressure for SmRu₄P₁₂,[6] making it impossible for $\Delta l/l$ to account for the change in C^0. As the slope change of C^0 happens mainly during the initial application of pressure, it may suggest some extrinsic influence of applying pressure on the sample system. Although this peculiarity is not well understood, it does not affect our analysis of the elastic softening at low temperatures with carefully estimated background, as will be shown later.

The temperature where a steep elastic drop occurs is known as the MI transition temperature T_{MI} at ambient pres-

sure. Similarly, all such anomalies observed under pressure are ascribed to MI transition. Although significant elastic softening is induced by hydrostatic pressure, the shape of the abrupt anomaly at T_{MI} shows no substantial change. In fact, electrical resistance under high pressures remains characteristic of MI transition up to at least 1.2 GPa, while the metallic behavior appears at $P > 3.5$ GPa.[25] T_{MI} increases when pressure is applied, in agreement with the observations in electrical resistance. This issue will be discussed later in terms of the Grüneisen parameter Ω. Unfortunately, we cannot detect an anomaly at T_N under pressure, as was successfully done in magnetic fields.[9]

IV. DISCUSSION

A. Pressure-induced elastic softening

Symmetrized strains induced by ultrasound perturb the CEF state via quadrupole-strain interaction $g_\Gamma O_\Gamma \epsilon_\Gamma$. Taking the intersite quadrupole interaction $g'_\Gamma O_\Gamma \langle O_\Gamma \rangle$ into account, elastic constant C_Γ can be formulated by the second derivative of the free energy as follows:

$$C_\Gamma(T) = C^0_\Gamma(T) - \frac{N g_\Gamma^2 \chi_\Gamma(T)}{1 - g'_\Gamma \chi_\Gamma(T)}. \tag{2}$$

Here, $C^0_\Gamma(T)$ is the background elastic constant, N the number of R ions per unit volume, $\chi_\Gamma(T)$ the corresponding strain susceptibility calculated using the CEF scheme, and g_Γ and g'_Γ the coupling constants of the quadrupole-strain and quadrupole-quadrupole, respectively. $C_\Gamma(T)$ measures the diagonal (Curie term) and nondiagonal (Van-Vleck term) quadrupolar matrix elements, analogous to the magnetic susceptibility that measures magnetic dipole matrix elements.[26] Analyzing the experimental results by using $\chi_\Gamma(T)$, one experimentally obtains $|g_\Gamma|$ and g'_Γ.

At ambient pressure, no elastic softening was observed above T_{MI} for C_L and only very slight softening was observed for C_T. Generally, this indicates a very weak quadrupole-strain coupling g_Γ for the Γ_{67} quartet ground state. This is believed to be a signature of the complex multipolar ordering in phase II. On the other hand, a high degree of softening is observed under hydrostatic pressures, especially for C_T, giving evidence of the degeneracy of the CEF ground state with respect to quadrupole moment. Hydrostatic pressure induces elastic strain $\epsilon_B = \epsilon_{xx} + \epsilon_{yy} + \epsilon_{zz}$ that corresponds to bulk modulus C_B. ϵ_B has no direct coupling with symmetry quadrupole moment O_Γ; thus, it is not a direct reason for the enhanced elastic softening.

A crucial point in the physics of the enhanced elastic softening is determining, which of the two types of inherent quadrupole moments (Γ_3 or Γ_5) is responsible. The answer to this question may give direct insight into the OP symmetry of phase II; unfortunately, it cannot be clarified based on the present results on a polycrystalline sample. In contrast to the symmetrized transverse modes in a single crystal such as $(C_{11}-C_{12})/2$ and C_{44} that respectively corresponds to Γ_3- and Γ_5-type quadrupole moments, C_T and C_L in a polycrystalline sample reflect an average of different elastic modes. The former consists of C_{44} and $(C_{11}-C_{12})/2$, while the latter
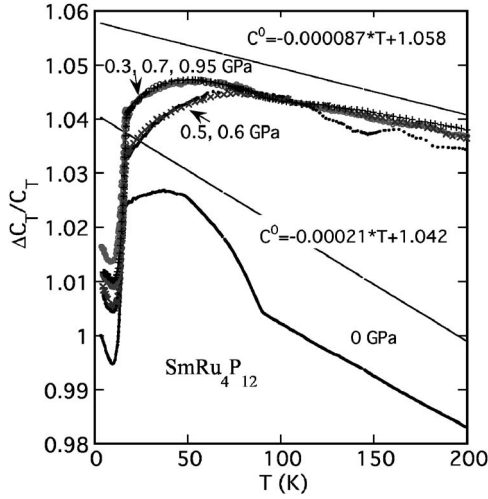
FIG. 3. Transverse elastic constant $C_T(T)$ under various pressures that is superposed on each other. The two solid lines indicate the estimated elastic background, described as $C^0 = -0.000\,21T + 1.042$ and $C^0 = -0.000\,087T + 1.058$, for 0 GPa and other nonambient pressures, respectively.

consists of all the available modes including C_{11} and bulk modulus C_B. For the same reason, Eq. (2) cannot be directly used to analyze elastic softening here. Nevertheless, as long as the $\chi_\Gamma(T)$ is dominated by the Curie term as predicted in the present system, Eq. (2) can be reformulated as follows:

$$C_\Gamma(T) = C_\Gamma^0(T) \left(\frac{T - T_C^0}{T - T_Q} \right). \tag{3}$$

According to Eq. (3), the quadrupole-strain coupling and intersite quadrupole interaction can be evaluated as an average. Furthermore, transforming Eq. (3) into Eq. (4) is helpful in the actual analysis.

$$\frac{1}{C_\Gamma^0(T) - C_\Gamma(T)} \approx \frac{T - T_Q}{T_C^0 - T_Q}. \tag{4}$$

Here, $T_Q = g_\Gamma' |\langle \varphi_i | O_\Gamma | \varphi_i \rangle|^2$ indicates the intersite quadrupole interaction. The difference of the two characteristic temperatures, $T_C^0 - T_Q = N g_\Gamma^2 |\langle \varphi_i | O_\Gamma | \varphi_i \rangle|^2 / C_\Gamma^0$, is usually termed the Jahn-Teller coupling energy E_{JT},[27] and is a function of quadrupole-strain coupling.

Before analyzing elastic softening, the elastic background $C^0(T)$ should be carefully estimated. This process may affect the fitted values of T_Q and E_{JT} to some degree. Here, we employ the commonly used T-linear C^0. Figure 3 presents the measurement data of C_T and two estimated $C^0(T)$ lines. All the curves at nonambient pressures are superposed on each other and a common $C^0(T)$ is estimated for them. Significantly, we found the pressure dependences of T_Q and E_{JT} to be almost independent of $C^0(T)$ as long as a common background is employed, as shown in this figure. In fact, a shared slope of all $C_T(T)$ curves under nonambient pressures at temperatures over 100 K can be observed, supporting the
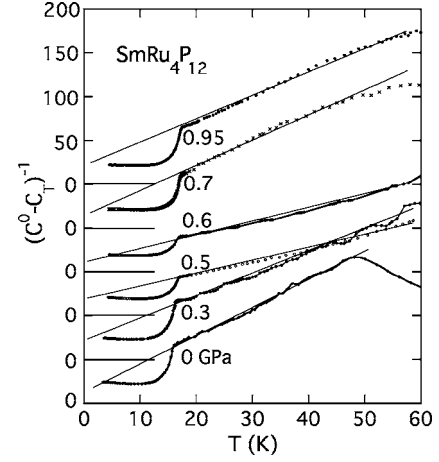

FIG. 4. $(C^0 - C_T)^{-1}$ as a function of temperature under various pressures. The solid lines are Curie term fits based on Eq. (4), which give values of T_Q and $E_{JT} = T_C^0 - T_Q$.

common $C^0(T)$. This procedure can maximally reduce extrinsic influence in estimating the two characteristic temperatures, and is crucial for the discussions later.

Figure 4 shows $(C^0 - C_T)^{-1}$ as a function of temperature. The T-linear increase above T_{MI} conforms to the Curie term described by Eq. (4) due to the Γ_3- and/or Γ_5-type quadrupole moment of the Γ_{67} ground state. The horizontal intercepts and the slopes of the linear fits give the quadrupolar interaction T_Q and the Jahn-Teller coupling energy E_{JT}. For longitudinal C_L, we performed the same procedure (not shown here). Note that the calculated curves shown in Figs. 1 and 2 are based on the obtained T_Q and E_{JT} values and Eq. (3).

Figure 5 presents the pressure dependence of the quadrupolar interaction, $-T_Q$ vs P. T_Q's are all negative, an indication of an antiferroquadrupolar interaction. T_Q is once enhanced by pressure; however, it is weakened again at around 0.7 GPa, where elastic softening is weakened. Shown in Fig. 6 are T_{soft} and Jahn-Teller energy E_{JT} as a function of pressure. Both of them depend on the same quadrupole-strain coupling and reflect the lattice instability. As expected, T_{soft} and E_{JT} show a similar pressure dependence. However, the
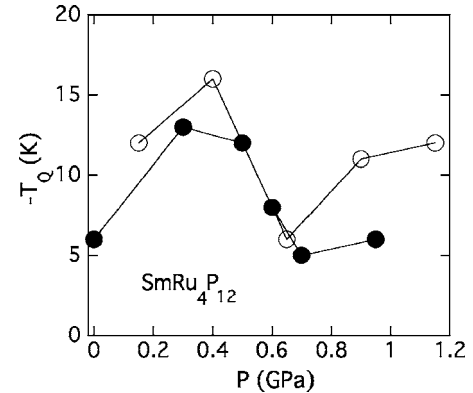

FIG. 5. Quadrupolar interaction T_Q as a function of pressure. The open circles denote data estimated from C_L and the solid circles from C_T.
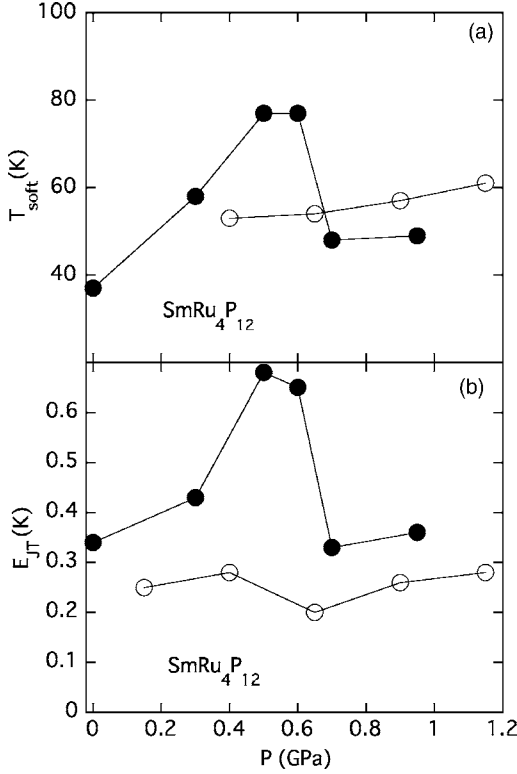
FIG. 6. Pressure dependences of (a) the temperature T_{soft} below which elastic softening appears and (b) the Jahn-Teller energy $E_{\text{JT}} = T_C^0 - T_Q$. The open circles denote data estimated from C_L and the solid circles from C_T.

two energies exhibit different pressure dependences for C_T and C_L; enhanced values around 0.5–0.6 GPa are found in transverse C_T, while no distinct change is observed in longitudinal C_L.

Here, we first discuss the pressure dependence of T_Q and E_{JT}. Because $T_Q = g'_\Gamma |\langle \varphi_i | O_\Gamma | \varphi_i \rangle|^2$ and $E_{\text{JT}} = N g_\Gamma^2 |\langle \varphi_i | O_\Gamma | \varphi_i \rangle|^2 / C_\Gamma^0$, two possible explanations of their pressure dependences are available. (1) The two energies change with pressure due to changes in the quadrupole moment $|\langle \varphi_i | O_\Gamma | \varphi_i \rangle|$. (2) Their changes are due to g'_Γ and g_Γ, respectively. For case (1), one expects a similar pressure dependence of T_Q and E_{JT}. This is different from our observations. Moreover, a significant change of the CEF scheme and the consequent quadrupole moment are not anticipated under the present hydrostatic pressures. The quadrupole Kondo effect may have an influence on $|\langle \varphi_i | O_\Gamma | \varphi_i \rangle|$, but one would expect a screened quadrupole moment by applying pressure, not an enhanced one. Thus, it seems likely that changes in g'_Γ and g_Γ account for the characteristic energies under pressure. Because $g'_\Gamma \sim T_Q$ is negative and $g_\Gamma^2 \sim E_{\text{JT}}$ is positive as factors in Eq. (2), the rapid decline of $|T_Q|$ and enhancement of E_{JT} around 0.5–0.6 GPa will enhance elastic softening, consistent with the experimental facts in C_T. The absence of enhanced E_{JT} in C_L within the present experimental accuracy remains an open question. Besides the hardness of C_L, which prevents a precise analysis of elastic softening, the difference between C_T and C_L may also suggest that the softening is due to one of the possible quadrupole modes, Γ_3 or Γ_5, but not to both.
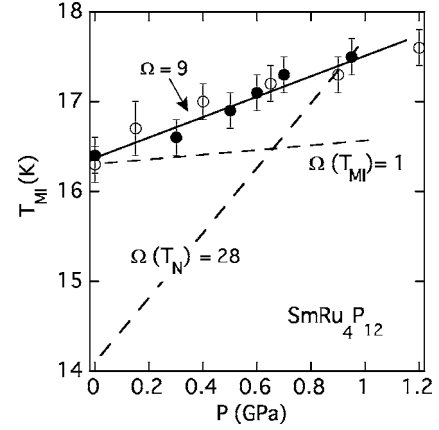

FIG. 7. T_{MI} as a function of pressure. The solid and open circles denote T_{MI} observed in C_T and C_L, respectively. The solid line is a guide for the eyes and represents a Grüneisen parameter of $\Omega = 9$. The broken lines represent two supposed pressure dependences for T_N ($\Omega = 28$) and T_{MI} ($\Omega = 1$), respectively.

B. Increase of T_{MI} with large Grüneisen parameter

Our results show that T_{MI} increases with pressure (Fig. 7), consistent with the observations of electrical resistance.[25] It is also in agreement with thermal expansion measurements where lattice shrinkage is observed below T_{MI}.[6] The monotonic increase of T_{MI} with pressure contrasts strikingly with the unusual changes in T_Q and E_{JT}, suggesting again that the MI transition is not a quadrupolar ordering. Comparatively, no obvious pressure dependence[28] or a very slight increase[29] was observed for the T_{AFQ} in the typical AFQ compound CeB$_6$. Formula (5) defines the Grüneisen parameter as a volume derivative of the phase-transition temperature,

$$\Omega = -\frac{\ln T_{\text{MI}}}{\ln V} = \frac{C_B}{T_{\text{MI}}} \frac{\partial T_{\text{MI}}}{\partial P}. \tag{5}$$

Based on this formula, the Grüneisen parameter Ω for T_{MI} is estimated to be 9 (solid line in Fig. 7). The pressure dependence of T_{MI} reported in Ref. 25 leads to an Ω of 7, roughly in agreement with ours. It is significant to make a comparison between the $\Omega(T_{\text{MI}})$ of SmRu$_4$P$_{12}$ and PrRu$_4$P$_{12}$. Performing the same calculation using the reported bulk modulus $C_B = 207$ GPa (Ref. 30) and the pressure dependence of T_{MI},[31] we obtain $\Omega(T_{\text{MI}}) \simeq 2$ for PrRu$_4$P$_{12}$. The $\Omega(T_{\text{MI}})$ for PrRu$_4$P$_{12}$ is a normal value, while that for SmRu$_4$P$_{12}$ is large, again reflecting the essential difference between the two MI transitions.

The considerably large Ω is reminiscent of the two very different Grüneisen parameters estimated for T_{MI} and T_N.[23] The conventional equation $\Omega = C_B \beta / C$ (here, β is the volume thermal expansion coefficient and C the specific heat) gives a huge $\Omega = 28$ for T_N, but a normal $\Omega = 1$ for T_{MI}. Widely different Ω's are expected to produce widely different pressure dependences of T_{MI} and T_N, as indicated by the broken lines in Fig. 7. Unfortunately, no magnetic fields were applied in this work, so T_{MI} and T_N are not separated and a more detailed P-T phase diagram is not available. Noticeably, the $\Omega = 9$ estimated in this work is smaller than that of T_N (Ω

=28) and larger than that of T_{MI} ($\Omega=1$). This is evidence that the pressure dependence of T_{MI} derived from our measurements depends, not only on the probable multipole OP in phase II, but also on the magnetic OP in phase III. Instead, we think that separating T_N and T_{MI} under pressure is much more difficult than at ambient pressure due to the enhanced interplay between the two phases. In addition, the origin of the enormous $\Omega(T_N)$ may be approachable by HF behaviors. A large Grüneisen parameter is usually observed in HF systems,[32] reflecting the large volume effect of the quasi p-f hybridization band. Indeed, Kondo behaviors (e.g., the $-\ln T$ dependence of electrical resistivity) are observed in $SmRu_4P_{12}$ below 50 K,[3] and elastic softening at low temperatures (below 3 K) similar to HF behavior is also observed.[23]

A strong interplay between phases II and III suggested by the large Ω hints at an octupole scenario for T_{MI} in $SmRu_4P_{12}$. This is clear because an octupole is magnetic, the same as the dipole OP in phase III, while the quadrupole is nonmagnetic and holds TRS. In fact, a mix between OP of phase II (octupole) and OP of phase III (dipole) is proposed in order to explain the obscurity of the II-III phase transition in Ref. 14. Noticeably, enhanced elastic softening under pressure indicates that quadrupole moment is one of the possible OPs in phase II or III under hydrostatic pressure. This inference may be extrapolated to ambient pressure where weak elastic softening appears. We infer two possibilities for this enhanced elastic softening. First, quadrupole ordering is induced or enhanced by pressures in phase II other than the primary OP, so $|g_\Gamma|$ and thus elastic softening is enhanced by quadrupole fluctuation. Second, quadrupole ordering is induced or enhanced in phase III besides the magnetic dipole. Considering that T_N may approach T_{MI} as anticipated from the Grüneisen parameter analysis, the second inference will also produce enhanced elastic softening. There are three kinds of multipole ordering available in the Γ_{67} ground state,[33] i.e., magnetic dipole, electric quadrupole, and magnetic octupole. Of these, octupole ordering may inherently induce quadrupole ordering ingredients, as in NpO_2,[18] or may induce quadrupole ordering by the mode-mixing effect[14,34] or by other mechanisms. Thus, induced quadrupole OP in phase II or III supports an octupole scenario for the MI transition. On the other hand, the largest elastic softening at

around 0.5–0.6 GPa means a kind of criticality between the two transitions at this pressure, considering the very different Grüneisen parameters. In fact, the virtual temperature dependences of T_{MI} and T_N based on the Grüneisen parameters (broken lines in Fig. 7) cross at the same pressure. When increasing the pressure, the system presumably moves away from the criticality state, and consequently the quadrupole-strain coupling and quadrupole fluctuation weaken again. This argument needs to be checked theoretically. Here, it should be noted that we did not observe clear signs that T_N exceeds T_{MI} under pressure. So the trends of the two phase-transition temperatures at pressures higher than the criticality remain an open question.

V. SUMMARY

To summarize, we measured the longitudinal elastic constant C_L and transverse elastic constant C_T for polycrystalline $SmRu_4P_{12}$ under hydrostatic pressure. Significant elastic softening is induced by hydrostatic pressure, especially in the transverse C_T. The results give evidence of the degeneracy of the CEF ground state with respect to quadrupole moments. The enhanced elastic softening indicates that quadrupole moment may be one of the possible OPs in phase II or phase III. The MI transition is found to increase by applying pressure with a large Grüneisen parameter of 9. We also found that elastic softening above T_{MI} has a strange pressure dependence. The greatest elastic softening is observed at around $P=0.5$–0.6 GPa, where the Jahn-Teller energy E_{JT} shows the largest values and $|T_Q|$ decreases. This strangeness may be related to the enormous Grüneisen parameter of T_N, in contrast to that of T_{MI}, and suggests a strong interplay between phases II and III. Our results prefer the octupole moment as the primary OP in phase II. Experiments in magnetic fields, with pressure applied simultaneously, are currently in progress, in order to separate the two successive transitions and establish a detailed P-H-T phase diagram.

*Electronic address: yoshizawa@iwate-u.ac.jp

[1] E. D. Bauer, N. A. Frederick, P. -C. Ho, V. S. Zapf, and M. B. Maple, Phys. Rev. B **65**, 100506(R) (2002).

[2] S. Sanada, Y. Aoki, H. Aoki, A. Tsuchiya, D. Kikuchi, H. Sugawara, and H. Sato, J. Phys. Soc. Jpn. **74**, 246 (2005).

[3] C. Sekine, T. Uchiumi, I. Shirotani, and T. Yagi, in *Science and Technology of High Pressure*, edited by M. H. Manghnani, W. J. Nellis, and M. F. Nicol (Universities Press, Hyderabad, 2000), p. 826.

[4] K. Matsuhira, Y. Hinatsu, C. Sekine, T. Togashi, H. Maki, I. Shirotani, H. Kitazawa, T. Takamasu, and G. Kido, J. Phys. Soc. Jpn. **71**, 237 (2002) suppl.

[5] C. Sekine, I. Shirotani, K. Matsuhira, P. Haen, D. De Brion, G. Chouteau, H. Suzuki, and H. Kitazawa, Acta Phys. Pol. B **34**, 983 (2003).

[6] C. Sekine, Y. Shimaya, I. Shirotani, and P. Haen, J. Phys. Soc. Jpn. **74**, 3395 (2005).

[7] J. M. Effantin, J. Rossat-Mignod, P. Burlet, H. Bartholin, S. Kunii, and T. Kasuya, J. Magn. Magn. Mater. **47&48**, 145 (1985).

[8] K. Takegahara, H. Harima, and A. Yanase, J. Phys. Soc. Jpn. **70**, 1190 (2001).

[9] M. Yoshizawa, Y. Nakanishi, T. Kumagai, M. Oikawa, C. Sekine, and I. Shirotani, J. Phys. Soc. Jpn. **73**, 315 (2004).

[10] M. Yoshizawa, Y. Nakanishi, T. Kumagai, M. Oikawa, S. R. Saha,

H. Sugawara, and H. Sato, Physica B **359–361**, 862 (2005).

[11] S. Nakamura, T. Goto, S. Kunii, K. Iwashita, and A. Tamaki, J. Phys. Soc. Jpn. **63**, 623 (1994).

[12] Y. Nemoto, T. Yanagisawa, K. Hyodo, T. Goto, S. Miyata, R. Watanuki, and K. Suzuki, Physica B **329–333**, 641 (2003).

[13] K. Matsuhira, Y. Doi, M. Wakeshima, Y. Hinatsu, H. Amitsuka, Y. Shimaya, R. Giri, C. Sekine, and I. Shirotani, J. Phys. Soc. Jpn. **74**, 1030 (2005).

[14] M. Yoshizawa, Y. Nakanishi, M. Oikawa, C. Sekine, I. Shirotani, S. R. Saha, H. Sugawara, and H. Sato, J. Phys. Soc. Jpn. **74**, 2141 (2005).

[15] K. Hachitani, H. Fukazawa, Y. Kohori, I. Watanabe, C. Sekine, and I. Shirotani, Phys. Rev. B **73**, 052408 (2006).

[16] S. Masaki, T. Mito, N. Oki, S. Wada, and N. Takeda, J. Phys. Soc. Jpn. **75**, 053708 (2006).

[17] S. Tsutsui, Y. Kobayashi, T. Okada, H. Haba, H. Onodera, Y. Yoda, M. Mizumaki, H. Tanida, T. Uruga, C. Sekine, I. Shirotani, D. Kikuchi, H. Sugawara, and H. Sato, J. Phys. Soc. Jpn. **75**, 093703 (2006).

[18] J. A. Paixão, C. Detlefs, M. J. Longfield, R. Caciuffo, P. Santini, N. Bernhoeft, J. Rebizant, and G. H. Lander, Phys. Rev. Lett. **89**, 187202 (2002).

[19] C. Sekine, T. Uchiumi, I. Shirotani, and T. Yagi, Phys. Rev. Lett. **79**, 3218 (1997).

[20] C. H. Lee, H. Matsuhara, A. Yamamoto, T. Ohta, H. Takazawa, K. Ueno, C. Sekine, I. Shirotani, and T. Hirayama, J. Phys.: Condens. Matter **13**, L45 (2001).

[21] H. Harima and K. Takegahara, Physica B **312–313**, 843 (2002).

[22] K. Iwasa, L. Hao, T. Hasegawa, T. Takagi, K. Horiuchi, Y. Mori, Y. Murakami, K. Kuwahara, M. Kohgi, H. Sugawara, S. R.

Saha, Y. Aoki, and H. Sato, J. Phys. Soc. Jpn. **74**, 1930 (2005).

[23] M. Yoshizawa, Y. Nakanishi, T. Tanizawa, A. Sugihara, M. Oikawa, P. Sun, H. Sugawara, S. R. Saha, D. Kikuchi, and H. Sato, Physica B **378–380**, 222 (2006).

[24] T. Goto, Y. Nemoto, K. Sakai, T. Yamaguchi, M. Akatsu, T. Yanagisawa, H. Hazama, K. Onuki, H. Sugawara, and H. Sato, Phys. Rev. B **69**, 180511(R) (2004).

[25] A. Miyake, I. Ando, T. Kagayama, K. Shimizu, C. Sekine, K. Kihou, and I. Shirotani, J. Alloys Compd. **408-412**, 238 (2006).

[26] P. Thalmeier and B. Lüthi, in *Handbook on the Physics and Chemistry of Rare Earths*, edited by K. A. Gschneidner, Jr. and L. Eyring (North-Holland, Amsterdam, 1991), Vol. 14.

[27] K. I. Kugel and D. I. Khomskii, Usp. Fiz. Nauk **136**, 621 (1982) [Sov. Phys. Usp. **25**, 231 (1982)].

[28] S. Sullow, V. Trappe, A. Eichler, and K. Winzer, J. Phys.: Condens. Matter **6**, 10121 (1994).

[29] Y. Uwatoko, K. Kosaka, M. Sera, and S. Kunii, Physica B **281&282**, 555 (2000).

[30] I. Shirotani, J. Hayashi, T. Adachi, C. Sekine, T. Kawakami, T. Nakanishi, H. Takahashi, J. Tang, A. Matsushita, and T. Matsumoto, Physica B **322**, 408 (2002).

[31] A. Miyake, T. Kagayama, K. Shimizu, C. Sekine, K. Kihou, and I. Shirotani, Physica B **359-361**, 853 (2005).

[32] B. Lüthi and M. Yoshizawa, J. Magn. Magn. Mater. **63&64**, 274 (1987).

[33] R. Shiina, H. Shiba, and P. Thalmeier, J. Phys. Soc. Jpn. **66**, 1741 (1997).

[34] Y. Kuramoto and H. Kusunose, J. Phys. Soc. Jpn. **69**, 671 (2000).